Formation of Tetrahedron-Like Pores during Anodic Etching of (100) Oriented n-GaAs

S. Langa,[a,b,z] **J. Carstensen,**[a] **I. M. Tiginyanu,**[b] **M. Christophersen,**[a,*] **and H. Föll**[a,**]

[a]Faculty of Engineering, Christian-Albrechts-University, D-24143 Kiel, Germany
[b]Laboratory of Low-Dimensional Semiconductor Structures, Institute of Applied Physics, Technical University of Moldova, MD-2004 Chisinau, Moldova

The morphology of porous layers obtained by electrochemical etching of (100) oriented n-GaAs substrates in an aqueous solution of HCl was studied. At low anodic current densities, up to 5 mA/cm², pores in the form of triangular prisms grew along ⟨111⟩ crystallographic directions. For larger current densities the shape of the pores did not suffer any changes at the beginning of the process, while after a definite period of time the morphology of pores changed drastically to chains of tetrahedral voids with {111} facets.
© 2001 The Electrochemical Society. [DOI: 10.1149/1.1423803] All rights reserved.

After the discovery of the visible photoluminescence in porous Si,[1] pore formation in semiconductor materials received a great deal of attention from the scientific community. Electrochemical etching proved to be a powerful tool for developing 2D periodic dielectric structures which in turn can be used as photonic bandgap materials.[2] Over the last few years, much more information appeared concerning pore formation not only in n- and p-type Si but also in other semiconductors such as III-V compounds.[3-5] Porous structures of III-V materials are especially interesting because of their larger energy bandgap for electrons and well designed 2D or 3D periodic structures may allow fabrication of photonic crystals[6] with a photonic bandgap in the near infrared and visible region of the spectrum (*e.g.*, at $h\nu > 1.3$ eV), which is not possible with Si due to its small energy gap for electrons.

The mechanism of pore formation is moderately well understood in Si, which is the most investigated semiconductor material in this regard. While for Si several pore formation mechanisms were proposed[7-9] focusing on explaining the large variety of pores observed in this material, III-V semiconductors show peculiar features of their own. Nevertheless, it appears that some general principles such as the spatial distribution of the electric field[7] and preferential dissolution at defects[10,11] govern the process of electrochemical dissolution of these materials, too.

A subject of interest is the preferential orientation of pores along definite crystallographic directions. In n-GaAs, for instance, the pores were found to grow along ⟨111⟩ crystallographic directions and to expose (112) planes.[3,12] In this paper, we report on pores obtained in (100) oriented n-GaAs anodized at as high anodic current densities as to change considerably the morphology of the porous layer. While still growing along the ⟨111⟩ crystallographic directions, the pores consist of chains of overlapping tetrahedral voids which expose {111}A planes as facets. The observed pore morphology throws additional light on the mechanism of pore formation in III-V compounds.

The (100) oriented GaAs substrates used in this work were cut from the liquid-encapsulated-Czochralski grown Si-doped ingots with the electron concentration of 10^{17} cm^{-3} at $T = 300$ K. The anodization was carried out in an electrochemical double cell described elsewhere.[13] A four-electrode configuration was used; a Pt reference electrode in the electrolyte (RE), a Pt sense electrode on the sample (SE), a Pt counter electrode (CE), and a Pt working electrode (WE). The electrodes were connected to a specially manufactured potentiostat/galvanostat.

The electrolyte was pumped continuously through both parts of

the double cell by means of peristaltic pumps. The equipment used in the experiments was computer controlled. The area of the sample exposed to the electrolyte was 0.12 cm². The anodic etching was carried out using 5 and 10% HCl aqueous electrolytes at various current densities in the galvanostatic regime. After electrochemical etching, fresh cleavage surfaces were prepared and studied using a scanning electron microscope (SEM) operating at 14 kV.

Figure 1 illustrates an SEM image in cross section taken from a porous layer fabricated at a current density of 5 mA/cm². In this case, with the exception of the phase of pore nucleation, the monitored voltage (under galvanostatic control) between RE and SE electrodes has a relatively constant value during the whole duration of the experiment. Being oriented along ⟨111⟩ directions, the pores possess a well developed triangular prism-like shape (see the inset in Fig. 1) with {112} planes as facets. Pores with similar morphology were observed in GaAs earlier.[3,12]

However, the time behavior of the RE-SE voltage significantly changes when the current is sufficiently increased. After an initial interval of relatively constant voltage at the beginning of the etching process an increase in the voltage occurs. At the current density $j = 85$ mA/cm², for instance, a sharp voltage jump occurs after approximately 75 min of etching in 5% HCl. SEM investigations revealed that the voltage jump initiates a new phase of pore growth. Figure 2 shows SEM images in cross section taken from a sample anodized at a current density of 85 mA/cm². The pores shown were
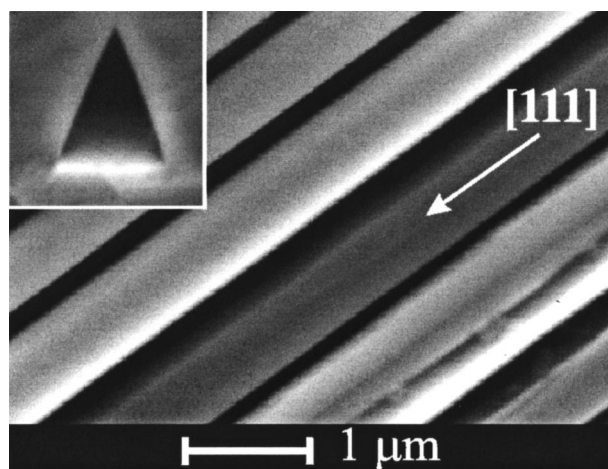

Figure 1. SEM in cross section taken from a porous layer anodized at low current densities; $j = 5$ mA/cm², HCl 5%. The inset illustrates the magnification of the shape of pores.
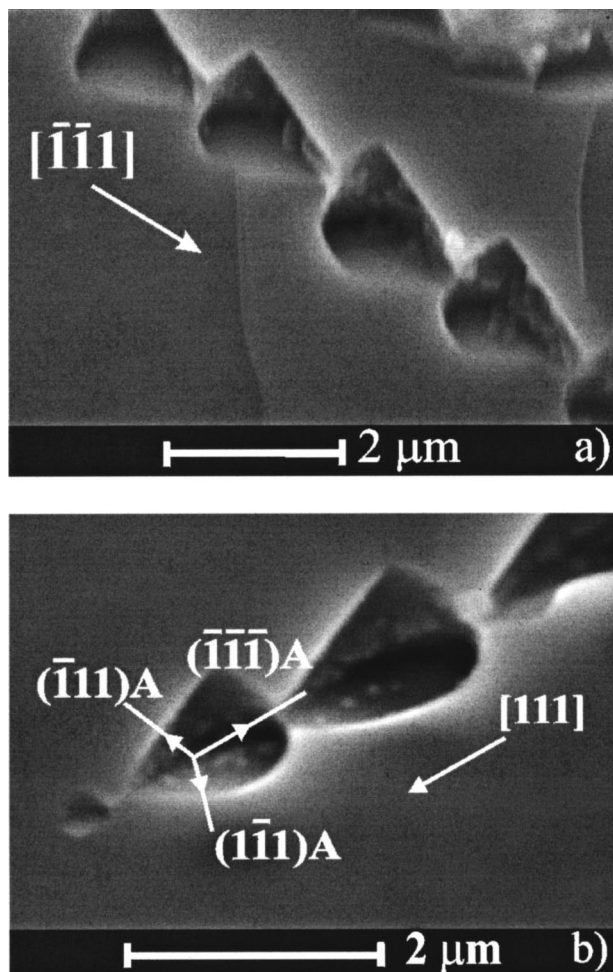
Figure 2. SEM in cross section taken from a porous layer after the voltage increase; $j = 85$ mA/cm^2, HCl 5%.

Figure 3. Schematic representation of the process explaining the tetrahedron-like pore formation according to the "aging" concept.

produced after the voltage jump and still form an angle of 54° with the normal to the surface. This means that they continue to grow along ⟨111⟩ crystallographic directions, like they did before the voltage jump. The pore walls, however, are not smooth anymore as those presented in Fig. 1, but form the aforementioned chains of interconnected tetrahedral voids. Three of the four facets of the tetrahedron can be easily observed in Fig. 2a and b.

Note that a similar morphology has been observed earlier in Si,[14] but instead of the tetrahedron-like voids, in Si an octahedron-like structure develops because the stopping planes as described below are different from those in GaAs. The current burst model[9] explains the octahedron-like pores observed in Si by means of the so-called aging of the pore walls. Aging in this case describes the passivation at pore tips with time as a function of current density. H-passivation hinders the oxidation of Si and is greatly dependent on crystallographic planes. {111} planes are most easily passivated and thus most stable against dissolution, therefore the octahedron-like pores expose them as stopping planes.

The observation of self-induced pore diameter oscillations with similar shapes in quite different semiconductors like Si and GaAs indicates that the general rules governing pore formation in these materials are not so different. Thus, we try to use the aging concept introduced for Si to explain the formation of the tetrahedron-like pores observed in GaAs taking into account that in GaAs it is Cl-passivation rather than H-passivation that impedes oxidation and thus the process of local dissolution.[15] Moreover, the stopping
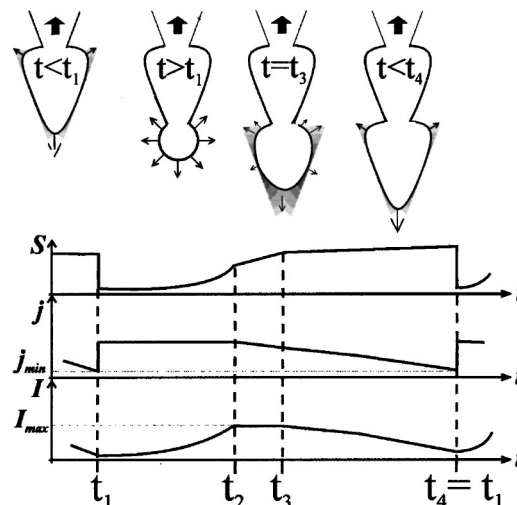
planes in this case are the so-called {111}A planes, *i.e.*, {111}Ga-rich planes. Therefore it is expected that the observed tetrahedron-chain pores expose these planes.

Briefly, the aging concept comprises the following basic principles. Current flow is supposed to be inhomogeneous in space and time, *i.e.*, there are current bursts followed by periods without charge transfer during which aging may occur. Passivation of pore tips is thus more pronounced at lower current densities because there is more quiescent time between current bursts. A schematic description of the process assumed to be responsible for the formation of tetrahedron-like pores is presented in Fig. 3.

Consider the situation when the current density at a pore tip (j_{tip}) has reached a critical low value j_{min} where nearly the whole surface of the pore tip (S_{tip}) is passivated ($t < t_1$ in Fig. 3). How the system reaches the critical current density is explained later. Keeping in mind that the experiments were performed in a galvanostatic regime the current must flow through the sample all the time and in any conditions. Thus, it can happen that to maintain a constant high current though the whole sample, the system will be forced to abandon a significant part of the strongly passivated surface of the tip and to concentrate the current flow only through a small area at the tip of the pore in order to increase the current density which in turn decreases significantly the passivation ($t = t_1$ in Fig. 3). Therefore on the diagram in Fig. 3 at $t = t_1$ sharp steps for S_{tip} (down) and j_{tip} (up) occur. The reason why the system chooses the small end of the tip is that here the electric field intensity is strengthened due to the curvature of the pore tip and is easier to break the passivation. Immediately after the moment t_1 a small spherical cavity at the tip of the pore is formed (see Fig. 2b). The cavity does not expose any crystallographic planes, no preferential passivation is present and the reaction in this stage can be considered to be kinetically controlled. This means that due to dissolution the surface of the sphere will increase with time in a quadratic manner (sphere), while the current density at the tip remains constant ($t_1 < t < t_2$). Consequently during this period of time the value of the current $I = jS$ will increase as the surface does. Nevertheless, taking into account that the tetrahedron-like pores begin to grow far underneath the surface, the current I will increase only up to a certain maximum value (I_{max}) which in fact is defined (limited) by diffusion of species (oxidizing, oxide dissolving, and reaction products) to and from the pore tips. Because I_{max} is the maximum current value which at this moment the system can carry through one pore, it will try to keep $I = I_{max}$ constant for a while ($t_2 < t < t_3$). Meantime the surface of the sphere will continue to grow (dissolution takes place). This

means that the current density starts to decrease its value and according to the current burst model the surface passivation on the contrary will increase. {111}A planes will be passivated more easily in our case. Thus, after the diffusion limited current is reached, the spherical cavity will begin to expose these planes ($t > t_2$) transforming itself in a tetrahedron cavity. The current density j_{tip} will continue to decrease until it reaches again the critical value and consequently a new step in S_{tip} and j_{tip} will occur ($t = t_4$), *i.e.*, a new tetrahedron begins to grow. As can be observed from Fig. 3, the current at pore tip I_{tip} also varies with time, the upper limit being I_{max}.

Note that in the current burst model developed for Si [9] one of the general assumptions is that the current at the pore tip also oscillates but due to a random shift in the oscillation phase at different pore tips a constant macroscopic current across the sample can be obtained.

Now the answer to the question why tetrahedron-like pores are observed only after a definite interval of time from the beginning of the experiment is relatively simple. Namely, at the beginning of the experiment the current density at pore tips is much higher than the critical value j_{min}, therefore the system needs some time before reaching it.

The second question is why the system can reach this critical value at pore tips only at high externally applied currents? It has been observed earlier that the pores initially nucleated at the surface of the sample are branching during the anodization process.[3] If a constant external current is applied to the sample, the current density at pore tips depends on the number of pores in the substrate. Thus, due to branching, the number of pore tips in the substrate increases in time, which means that the current density at the pore tips is not constant but decreases with time. Eventually, the decrease of j_{tip} with time allows the system to reach the critical j_{min} current density at pore tips which leads to the formation of linked tetrahedrons as explained above. At low values of the external current the branching effect is practically absent or is very insignificant, therefore, the number of pore tips is constant in time and so does the current density at the tips, *i.e.*, it cannot decrease to the critical value where the tetrahedron pores begin to grow.

To test the assumptions made above, the influence of electrolyte concentration and current density on the time interval from the beginning of the experiment until tetrahedron-like pores begin to grow was studied. Figure 4 shows the time dependence of the voltage at different current densities for two electrolyte concentrations, 5% HCl (Fig. 4a) and 10% HCl (Fig. 4b). The time needed to reach the tetrahedron regime of pore growth shortens both with increasing current density and electrolyte concentration.

These observations can be explained as follows. Concentrated electrolytes mean a higher number of Cl^- ions in solution. Thus, the number of passivated bonds which can form per unit of time is larger as compared with more diluted electrolytes. Comparable passivation states (equal number of passivated bonds on surface unit) for two different concentrations of the electrolyte $c_1 < c_2$, are obtained for two different current densities $j_1 < j_2$ that must flow through pore tips. Consequently, the critical value j_{min} will be higher in more concentrated solutions ($j_{min1} < j_{min2}$). As explained above, the actual current density at pore tips decreases in time (due to branching) from the initial value j_{init} at the surface of the sample until j_{min} is reached and the system enters a new state (voltage jump). So, the time needed to reach j_{min2} is shorter than that required to reach j_{min1} because $j_{init} - j_{min2} < j_{init} - j_{min1}$. This is in good agreement with the results presented in Fig. 4a and b.

The decrease of the time necessary for the system to reach the tetrahedron regime when increasing the externally applied current density can be explained taking into account the fact that branching of pores occurs more frequently at high externally applied currents and is practically absent at low currents. Thus, j_{tip} decreases faster at high than at low values of the externally applied current. Consequently, j_{min} is reached in a shorter period of time.
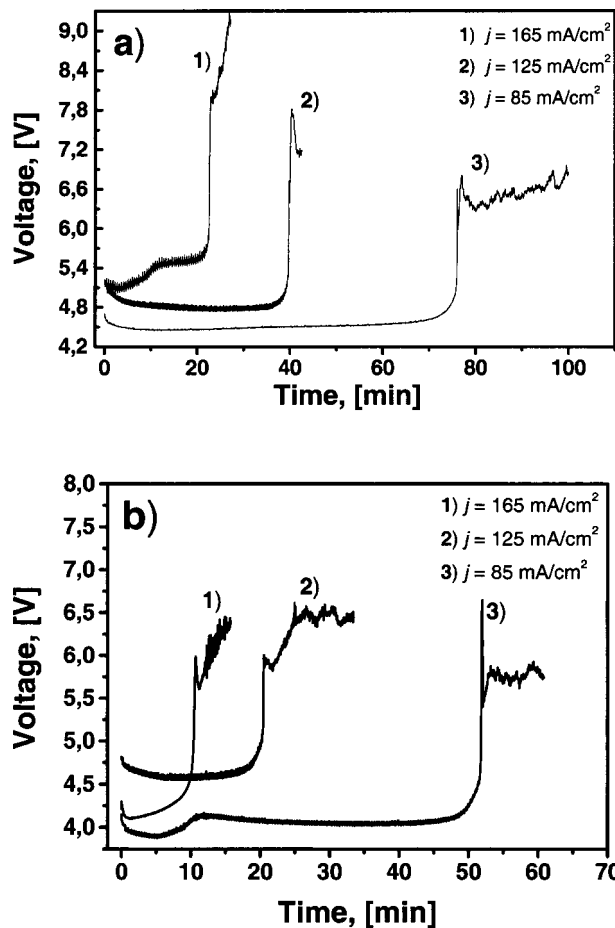

Figure 4. Time dependence of voltage at different current densities. (a) HCl 5% and (b) HCl 10%.

The observed architecture of pores offers new insights into the mechanism of pore formation in GaAs, and also represents an interesting structure for practical applications. The pores obtained at high current densities after the voltage jump look like asymmetrically modulated microchannels and, according to the new concept of drift ratchet[16,17] are suitable for designing micropumps to separate micrometer-size particles dissolved in liquids.

In conclusion, at low current densities the pores in n-GaAs grow along $\langle 111 \rangle$ crystallographic directions. Branching is insignificant and, consequently, the actual current density at pore tips is nearly constant during the whole experiment. At high externally applied current branching occurs very often, thus the actual current density at pore tips decreases in time and j_{min} can be reached after a certain period of time from the beginning of the experiment. The compromise between the current flow and tips passivation leads to a totally new morphology of the pores, namely, the formation of tetrahedron-like interconnected voids. The time required to reach the conditions for tetrahedron-like pore formation depends on the externally applied current and electrolyte concentration, which can be explained on the basis of aging concept.

References

1. L. T. Canham, *Appl. Phys. Lett.,* **57**, 1046 (1990).
2. J. D. Joannopoulos, R. D. Meade, and J. N. Winn, *Modeling the Flow of Light*, Princeton University Press, Princeton, NJ (1995).
3. F. M. Ross, G. Oskam, P. C. Searson, J. M. Macaulay, and J. A. Liddle, *Philos. Mag. A,* **75**, 525 (1997).
4. B. H. Erne, D. Vanmeakelbergh, and J. J. Kelly, *Adv. Mater.,* **7**, 739 (1995).
5. P. Schmuki, J. Fraser, C. M. Vitus, M. J. Graham, and H. Isaacs, *J. Electrochem. Soc.,* **143**, 3316 (1996).
6. U. Grüning, V. Lehmann, S. Ottow, and K. Busch, *Appl. Phys. Lett.,* **68**, 747 (1996).
7. H. Föll, *Appl. Phys. A,* **53**, 8 (1991).
8. B. H. Erne, D. Vanmeakelbergh, and J. J. Kelly, *J. Electrochem. Soc.,* **143**, 305 (1996).
9. J. Carstensen, M. Christophersen, and H. Föll, *Mater. Sci. Eng., B,* **69-70**, 23 (2000).
10. P. Schmuki, L. E. Erickson, D. J. Lockwood, J. W. Fraser, G. Champion, and H. J. Labbe, *Appl. Phys. Lett.,* **72**, 1039 (1998).
11. I. M. Tiginyanu, C. Schwab, J.-J. Grob, B. Prevot, H. L. Hartnagel, A. Vogt, G. Irmer, and J. Monecke, *Appl. Phys. Lett.,* **71**, 3829 (1997).
12. S. Langa, J. Carstensen, M. Christophersen, H. Föll, and I. M. Tiginyanu, *Appl. Phys. Lett.,* **78**, 1074 (2001).
13. S. Langa, I. M. Tiginyanu, J. Carstensen, M. Christophersen, and H. Föll, *Electrochem. Solid-State Lett.,* **3**, 514 (2000).
14. C. Jäger, B. Finkenberger, W. Jäger, M. Christophersen, J. Carstensen, and H. Föll, *Mater. Sci. Eng., B,* **69-70**, 199 (2000).
15. Z. H. Lu, F. Chatenoud, M. M. Dion, M. J. Graham, H. E. Ruda, I. Koutzarov, Q. Liu, C. E. J. Mitchell, I. G. Hil, and A. B. McLean, *Appl. Phys. Lett.,* **67**, 670 (1995).
16. Ch. Kettner, P. Reiman, P. Hänggi, and F. Müller, *Phys. Rev. E,* **61**, 312 (2000).
17. F. Müller, A. Birner, J. Schilling, U. Gösele, Ch. Kettner, and P. Hänggi, *Phys. Status Solidi A,* **182**, 585 (2000).